

Temporal metabolomic responses of cultured HepG2 liver cells to high fructose and high glucose exposures

John K. Meissen · Kristin M. Hirahatake ·
Sean H. Adams · Oliver Fiehn

Received: 6 May 2014 / Accepted: 8 September 2014 / Published online: 19 September 2014
© Springer Science+Business Media New York 2014

Abstract High fructose consumption has been implicated with deleterious effects on human health, including hyperlipidemia elicited through *de novo* lipogenesis. However, more global effects of fructose on cellular metabolism have not been elucidated. In order to explore the metabolic impact of fructose-containing nutrients, we applied both GC-TOF and HILIC-QTOF mass spectrometry metabolomic strategies using extracts from cultured HepG2 cells exposed to fructose, glucose, or fructose + glucose. Cellular responses were analyzed in a time-dependent manner, incubated in media containing 5.5 mM glucose + 5.0 mM fructose in comparison to controls incubated in media containing either 5.5 mM

glucose or 10.5 mM glucose. Mass spectrometry identified 156 unique known metabolites and a large number of unknown compounds, which revealed metabolite changes due to both utilization of fructose and high-carbohydrate loads independent of hexose structure. Fructose was shown to be partially converted to sorbitol, and generated higher levels of fructose-1-phosphate as a precursor for glycolytic intermediates. Differentially regulated ratios of 3-phosphoglycerate to serine pathway intermediates in high fructose media indicated a diversion of carbon backbones away from energy metabolism. Additionally, high fructose conditions changed levels of complex lipids toward phosphatidylethanolamines. Patterns of acylcarnitines in response to high hexose exposure (10.5 mM glucose or glucose/fructose combination) suggested a reduction in mitochondrial beta-oxidation.

John K. Meissen and Kristin M. Hirahatake contributed equally.

Electronic supplementary material The online version of this article (doi:10.1007/s11306-014-0729-8) contains supplementary material, which is available to authorized users.

J. K. Meissen · O. Fiehn (✉)
UC Davis West Coast Metabolomics Center, University of
California Davis, 451 Health Sciences Dr., Davis, CA 95616,
USA
e-mail: ofiehn@ucdavis.edu

K. M. Hirahatake · S. H. Adams
Department of Nutrition, University of California Davis,
One Shields Avenue., Davis, CA 95616, USA

K. M. Hirahatake · S. H. Adams
Obesity and Metabolism Research Unit, USDA-Agricultural
Research Service Western Human Nutrition Research Center,
430 W. Health Sciences Dr., Davis, CA 95616, USA

O. Fiehn
Department of Biochemistry, Faculty of Sciences,
King Abdulaziz University, PO Box 80203, Jeddah 21589,
Saudi-Arabia

Keywords High fructose corn syrup · Metabolic networks · Time-of-flight mass spectrometry · Chromatography · Lipidomics

1 Introduction

Very high intakes of fructose-containing sugars (FCS) have been linked with several adverse health effects in modern society (Bray et al. 2004; Havel 2005), with the caveat that the impact of more typical fructose intakes on health remain to be clarified. High fructose intake and hepatic metabolism results in a hyperlipidemic phenotype, a risk factor for cardiovascular disease characterized by an increase in circulating lipids and lipoproteins (Fried and Rao 2003; Hallfrisch et al. 1983; Parks and Hellerstein 2000; Rizkalla 2010), and high fructose consumption has been implicated in the development of insulin resistance, a

risk factor for cardiovascular disease and diabetes (Beck-Nielsen et al. 1980; Daly et al. 1997; Elliott et al. 2002). The correlation between increases in obesity and high fructose corn syrup consumption in the United States, as well as differences in metabolism from glucose, have also led some to speculate that fructose metabolism may represent a factor contributing to the recent rise in obesity (Bray et al. 2004). While these adverse health effects are certainly a combination of several factors, including total caloric intake and physical activity patterns, unraveling the metabolic impact of fructose can enhance our understanding of its putative relationship with metabolic health and facilitate development of effective public policy guidelines. Current progress in elucidating the effects of fructose consumption has been reviewed in the literature (Fried and Rao 2003; Havel 2005; Parks and Hellerstein 2000; Rizkalla 2010).

The major site of fructose metabolism is the liver (Mayes 1993; Mendeloff and Weichselbaum 1953; Topping and Mayes 1971). Fructose is phosphorylated by fructokinase to form fructose-1-phosphate, which is converted into the glycolysis metabolites dihydroxyacetone phosphate and glyceraldehyde-3-phosphate (Heinz et al. 1968; Mayes 1993). Entry into glycolysis in this intermediate stage is a notable difference from glucose metabolism as it bypasses phosphofructokinase, a major regulatory point in glycolysis (Underwood and Newsholme 1965). Recently, we confirmed and extended these observations by determining the time course of hexose derivative concentrations and hexosamines in a HepG2 human hepatocyte cell model exposed to either glucose or glucose plus fructose (Hirahatake et al. 2011). Using data from that study, we here investigate metabolic effects in these cells in an untargeted metabolomics hypothesis-generating manner instead of hexosamine-targeted only. While the dominant pathway for fructose metabolism is known, the effect of fructose on the complex array of interconnected systems and regulatory mechanisms that constitutes cellular metabolism and its subsequent translation to phenotype remains unclear. Bypassing the major regulatory point of glycolysis may cause an increased availability of glycolysis metabolites, such as glycerol-3-phosphate and pyruvate. This increase could contribute to the hyperlipidemic phenotype as glycerol 3-phosphate and pyruvate are also lipid biosynthesis precursors (Mayes 1993). In addition, fructose promotes esterification of free fatty acids (Topping and Mayes 1972), inhibits hepatic lipid oxidation (Roglans et al. 2002; Topping and Mayes 1972; Vilà et al. 2011), and decreases levels of mitochondrial carnitine palmitoyltransferase 1 (Roglans et al. 2002; Vilà et al. 2011), the major regulatory enzyme of the fatty acid oxidation process (McGarry and Brown 1997; McGarry and Foster 1980). Increased activity of lipogenic enzymes, including fatty acid synthase and acetyl-CoA carboxylase,

contributes to the hyperlipidemic phenotype in rodents (Bruckdorfer et al. 1972; Koo et al. 2008; Spence and Pitot 1982; Winder et al. 1975), but to date the importance of this in human liver in response to fructose is largely unknown (Hirahatake et al. 2011).

Metabolomics is an ideal strategy to address the metabolic impact of fructose, especially when coupled to temporal observations, as this approach effectively characterizes the biochemical state of a particular cell type and delineates relevant changes when compared across experimental conditions (Fiehn 2002). Using multiple metabolomics platforms can yield a more global representation of differences between fructose and glucose metabolism than single platforms, providing clarity to known metabolic effects and revealing previously-unknown changes in cellular metabolism. One recently published report applied metabolomics to delineate changes in metabolite profiles in several rat tissues, including liver, between animals fed a high fructose diet and animals fed a standard chow diet (Lin et al. 2011). They reported significant effects on phosphatidylcholine (PC) and phosphatidylethanolamine (PE) lipid structures as well as free fatty acids in liver. Reportedly, the analyses also revealed significant changes in cytosine, malate, and ergothioneine levels (Lin et al. 2011).

Previously, we applied targeted mass spectrometry (MS) analysis to explore the impact of fructose on hexosamine biosynthesis with a HepG2 human liver cell model (Hirahatake et al. 2011). A particular challenge in metabolomics approaches is the quantitation of a wide array of structural classes such as complex lipids, carbohydrates, hydroxyl acids, amino acids, and nucleotide structures. No single analytical method can encompass such chemical diversity (Dettmer et al. 2007; Lei et al. 2011). We hence applied both gas chromatography time of flight (GC-TOF) MS and hydrophilic interaction chromatography quadrupole time of flight (HILIC-QTOF) MS methodologies to the aforementioned archived samples to expand metabolite coverage in order to expand the understanding of the impact of fructose on liver cell metabolism. HepG2 cells incubated in media containing 5.5 mM glucose + 5.0 mM fructose (Glc5Fru5) were compared to cell extracts from a control group incubated in media with 5.5 mM glucose (Glc5), a glucose concentration similar to human blood (Daly et al. 1998). While comparison of these two experimental conditions can reveal metabolic differences resultant of fructose addition, observed metabolic changes could also be caused by increased hexose resources. Therefore, a third condition containing 10.5 mM glucose (Glc10) was included to enable differentiation of metabolic effects caused by fructose from metabolic effects caused by increased hexose resources. Cells were acclimated to their respective media condition for 48 h prior to collection of

sample material to obtain a metabolite profile representative of continued exposure instead of response to a sudden change in carbohydrate resources. Sample material was collected at multiple time points to identify any potential sampling time related bias. Moreover, the time-course study design ensured that cells were able to adapt to a high-carbohydrate environment in which all gene regulation and post-translational modifications had taken place. The media exchange ensured to exclude potential build-up of excreted compounds. This temporal study design mimicked the highly dynamic metabolic response by intake of food in humans: we eat food in pulses (batch-wise) and lack constant nutritional environments, unlike continuously fed microbial industry fermenters. Nevertheless, results from any cell culture study need to be interpreted with caution, because cell cultures lack endocrine signaling of a multicellular tissue-dependent response. All annotated structures were incorporated into metabolite networks describing chemical similarity, biological relationships, magnitude of fold change between experimental conditions, and statistical significance. We hypothesized that fructose exposure would increase indices of *de novo* lipogenesis and lead to accumulation of metabolites marking reduced fatty acid β -oxidation.

2 Materials and methods

2.1 Cell culture and extraction

Growth of cell cultures was performed as described previously (Hirahatake et al. 2011). HepG2 cells (ATCC HB-8065) were cultured in MEM containing 10 % (v:v) FBS, 100 U/mL penicillin and 100 mg/mL streptomycin (Invitrogen, Carlsbad, CA), 1 x MEM non-essential amino acids, and 5.5 mM glucose at 37 °C in a 5 % CO₂ environment. Cells were grown for four to six passages in 10 cm tissue culture dishes with 14 mL MEM, and transferred to MULTIWELL™ 12 well culture dishes for incubation in 2 mL of the treatment medium. Upon reaching 80 % confluency, the cell culture medium was changed to media representative of experimental condition: 5.5 mM glucose MEM, 5.5 mM glucose MEM + 5 mM glucose, or 5.5 mM glucose MEM + 5 mM fructose. Media was replenished after 24 and 48 h. Cell material was collected at 10 min, 1, 6, and 24 h time points following the 48 h media replacement. Culture dishes were placed on ice and each well was washed twice with 1 mL ice-cold PBS. 4 mL ice-cold 3:1 methanol/H₂O extraction solvent was added to each well. Cell material was manually scraped from each well, and the extraction solvent cell material suspension was transferred to collection tubes and frozen at -80 °C prior to further processing.

Sample material was thawed on ice, vortexed for 20 s, sonicated for 5 min with a VWR 50HT Ultrasonic Bath (VWR International Inc., Bridgeport, NJ), and separated into 500 μ L aliquots. Each aliquot was centrifuged for 5 min @ 14,000 rcf, and supernatant was collected and lyophilized to dryness. Samples were kept on ice and removed only for sonication, centrifugation, and lyophilization steps. Lyophilized material was used for HILIC-QTOF metabolite profiling without additional clean-up steps. Lyophilized material for GC-TOF analysis was redissolved in 1:1 acetonitrile/H₂O, vortexed for 10 s, and centrifuged for 5 min @ 14,000 rcf. Supernatant was collected and lyophilized to dryness.

2.2 GC-TOF MS based metabolomics

Sample material representing six replicates of all experimental conditions were derivatized and analyzed as reported previously (Fiehn et al. 2010; Kind et al. 2009). A set of thirteen C8–C30 fatty acid methyl ester internal standards were added and samples were derivatized by the addition of 10 μ L methoxyamine hydrochloride in pyridine followed by 90 μ L MSTFA for trimethylsilylation of acidic protons.

A Gerstel MPS2 automatic liner exchange system (Gerstel GMBH & Co.KG, Mülheim an der Ruhr, Germany) was used to inject 0.5 μ L of sample at 50 °C (ramped to 250 °C) in splitless mode with 25 s split less time. Analytes were separated using an Agilent 6890 gas chromatograph (Agilent Technologies, Santa Clara, CA) equipped with a 30 m long, 0.25 mm i.d. Rtx5Sil-MS column with 0.25 mm 5 % diphenyl film and an additional 10 m integrated guard column (Restek, Bellefonte PA). Chromatography was performed with a constant flow of 1 mL/min while ramping the oven temperature from 50 to 330 °C with 22 min total run time. MS was performed with a Leco Pegasus IV time of flight mass spectrometer (Leco Corporation, St. Joseph, MI) with a 280 °C transfer line temperature, an electron ionization voltage of 70 eV, and an ion source temperature of 250 °C. Mass spectra were acquired between 85 and 500 m/z with a scan rate of 17 spectra/sec.

Result files were exported to our servers and further processed by our metabolomics BinBase database (Fiehn et al. 2005). All database entries in BinBase were matched against the Fiehn mass spectral library of 1,200 authentic metabolite spectra using retention index and mass spectrum information or the NIST05 commercial library. Peak heights of quantifier ions defined for each metabolite in BinBase were normalized to the average sum of intensities of all replicates in an experimental condition divided by the sample sum of intensities. External 5-point calibration

curves established with quality control mixtures containing 30 metabolites controlled for instrument sensitivity.

2.3 HILIC-QTOF MS based metabolomics

Sample material representing five to six replicates of all experimental conditions was redissolved in 100 μ L initial LC gradient solvent and analyzed within 24 h. An Agilent 1200 Series HPLC system, equipped with an autosampler and a thermostatted column compartment maintained at 4 and 40 $^{\circ}$ C respectively, was used for chromatographic separation of 5 μ L sample material. HILIC analysis was performed with a Waters 1.7 μ m Acquity BEH HILIC 2.1 \times 150 mm column (Waters Corporation, Milford, MA). Mobile phase consisted of H₂O with 5 mM ammonium acetate and 0.2 % acetic acid (A) and 9:1 acetonitrile:H₂O with 5 mM ammonium acetate and 0.2 % acetic acid (B). The gradient method was: 0–4 min—100 % B, 4–12 min—linear gradient to 45 % B, and 12–20 min—45 % B. The column was re-equilibrated for 20 min following each sample run, and flow rate was constant at 0.25 mL/min throughout the gradient method and re-equilibration.

LC eluents were analyzed with an Agilent 6530 accurate-mass Q-TOF mass spectrometer equipped with an Agilent Jet Stream ESI source in positive ion mode. MS and MS/MS data were collected with a 0.25 s scan rate in both profile and centroid modes, and mass calibration was maintained by constant infusion of reference ions at 121.0509 and 922.0098 m/z. MS/MS data was generated utilizing data dependent MS/MS triggering with dynamic exclusion. Parent ions, with a minimum 1,000 signal intensity, were isolated with a 4 m/z isolation width, and a variable collision energy was applied based on parent ion m/z ($10 + 0.02 \text{ eV} \cdot \text{ion m/z}$). Ions were excluded from data dependent MS/MS analysis for 30 s following acquisition of three spectra.

Raw data files were converted to mzXML format with the Trapper mzXML conversion software and processed with the MZmine v2.0 data processing software to generate an aligned peak list with ion intensities (Pluskal et al. 2010). For MS/MS library annotation, raw data files were imported into Agilent Mass Hunter Qual software, and ions with associated MS/MS spectra were extracted with the Find by Auto MS/MS tool. Extracted ions were annotated with the Search Accurate Mass Library tool equipped with the METLIN library (Smith et al. 2005). Acylcarnitine structures were manually identified based on accurate mass and comparison of retention time to known acylcarnitine standards in quality control mixtures. Raw data files were also converted to mgf format with Agilent Mass Hunter Qual software and imported into the NIST MS Search program equipped with the NIST MS/MS library (Retrieved from <http://chemdata.nist.gov/mass-spc/msms-search/>) and LipidBlast for MS/MS based annotation (Kind et al. 2013). All MS/MS library

matches were manually confirmed and any annotation with greater than 1.5 mDa mass error was removed. Annotated structures were matched to the MS level aligned peak list based on mass and retention time to create a matrix of annotated compounds and peak intensities. Annotated ion intensities were normalized to the average sum of intensities of all replicates in an experimental condition divided by the sample sum of intensities. External quality control mixtures containing multiple acylcarnitine structures controlled for chromatography quality and instrument sensitivity.

2.4 MetaMapp network construction and visualization

Data sets from the GC-TOF MS and HILIC-QTOF MS platforms were integrated into a single data set. In case of duplicate compound detections by both platforms, the method with the greatest signal to noise ratio was selected for further data processing. Statistical analysis was performed with Statistica 9.0 software. Annotated structures were imported into the web-based PubChem chemical structural clustering tool (accessible at: <http://pubchem.ncbi.nlm.nih.gov>) to generate a pair-wise chemical similarity matrix. The matrix and CID-KEGG ID pairs for metabolites were used as input in MetaMapp software (accessible at: <http://metamapp.fiehnlab.ucdavis.edu>) for generation of Cytoscape network files in simple interaction format (Shannon et al. 2003). A threshold of 0.7 Tanimoto score was used to define the similarity cut-off among non-lipid metabolites, and a 0.85 Tanimoto score was used to define the similarity cutoff for lipid structures. A KEGG RPAIR reaction (Kanehisa et al. 2010) network graph was created using a single-metabolic step neighbor finding algorithm in MetaMapp (Barupal et al. 2012). The final network graphs were imported into Cytoscape and merged into a single network graph. Results of differential statistics generated using Statistica 9.0 software were converted into Cytoscape node attribute files and were imported into Cytoscape. The graph was visualized using a yED organic layout algorithm in Cytoscape. Fold change was mapped to node size, and direction was mapped to node color. Additional sampling time analysis plots were created from integrated GC-TOF and HILIC-QTOF data sets for selected metabolites in Microsoft Excel 2010.

3 Results and discussion

3.1 Overall metabolic phenotypes of HepG2 cells under different carbohydrate loads can be distinguished via multivariate statistical analyses

Analysis of cell extracts with the GC-TOF MS system enabled identification of 112 different metabolites using

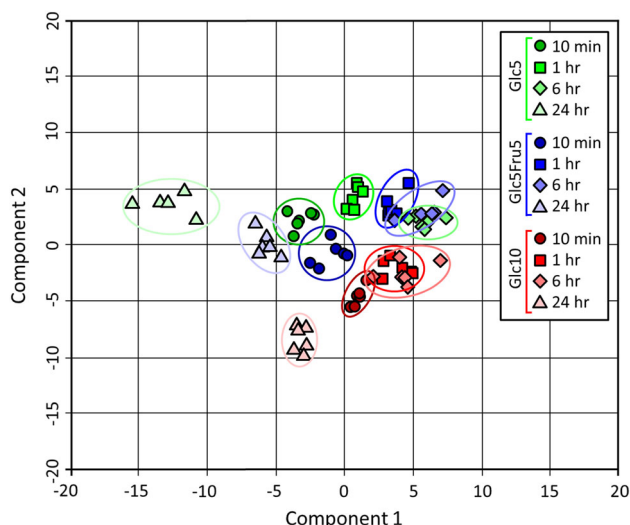


Fig. 1 Factor loadings plot from partial least square (PLS) multivariate analysis of 156 identified metabolites in HepG2 Cells. These loadings give the weight each metabolite had for forming the linear combination vectors of the PLS clustering of HepG2 cells grown under 5.5 mM glucose (Glc5), 10.5 mM glucose (Glc10) or 5.5 mM glucose and 5 mM fructose conditions (Glc5Fru5). The corresponding PLS clusters of the samples are shown in Supplementary Figure S1

the in-house BinBase database system (Kind et al. 2009). Complementary analysis with HILIC-QTOF mass spectrometry provided 54 additional metabolic annotations using the LipidBlast (Kind et al. 2013), METLIN and NIST MS/MS libraries. Integration of GC-TOF and HILIC-QTOF MS data sets yielded 156 unique annotations (Supplementary Table S1), representing many different compound classes including carbohydrates, sugar alcohols, sugar phosphates, hydroxyl acids, amino acids, purine and pyrimidine structures, free fatty acids, acylcarnitines, PCs and PEs.

Normalized ion intensities for the 156 unique annotations were used as input for partial least squares (PLS) multivariate statistics to assess the impact of carbohydrate structure and sampling time on the metabolite profiling data set (Fig. 1). The PLS model was selected to create a preliminary overview of metabolite profiles because it focuses on the biologically significant variance that distinguishes experimental conditions (Fiehn et al. 2008). While PLS analysis can potentially over-fit data sets generating separation of classes lacking significant variance (Westerhuis et al. 2008), subsequent univariate analysis confirmed many biologically significant differences between classes legitimizing application of the PLS approach. Separation of classes by component 1 was dominated by the time course of metabolism following exposure to fresh hexose media. In contrast, PLS component 2 separated the 10.5 mM glucose (Glc10) treatment sample groups from those classes that used 5.5 mM each of

glucose and fructose (Glc5Fru5) as a carbon source or that used only 5.5 mM glucose (Glc5). Interestingly, the Glc5 data presented a greater separation from Glc10 results than the Glc5Fru5 results, suggesting that addition of excess glucose may constitute a more substantial influence on HepG2 metabolite profiles than addition of comparable amounts of fructose. The PLS analysis also indicated that sampling time was a major factor influencing metabolite profiles and hence, must be considered in interpretation. The 24 h time point in particular displayed substantial separation from other time points while the 10 min, 1, and 6 h time points were more similar to each other within a specific treatment group. We have therefore focused our interpretations on early metabolic effects of different carbohydrate loads.

While application of the in-house BinBase database and several MS/MS libraries enabled annotation of 156 unique structures, approximately 800 features extracted from GC-TOF and HILIC-QTOF data files could not be annotated to specific metabolite structures (i.e. “unknowns”). PLS analysis of these unknown metabolites (Supplementary Figure S1) indicated many of the same trends observed in the PLS analysis of annotated metabolites. This observation shows that most unidentified peaks must be regarded as genuine metabolites produced by the HepG2 cells and under control of the same cellular events. The fact that so many genuine metabolites exist that cannot be annotated by comparison to known chemical structures indicates that our understanding of metabolic biochemistry is incomplete, and that many further enzymatic reactions will need to be elucidated before we can perform theoretical metabolic modeling of HepG2 cells.

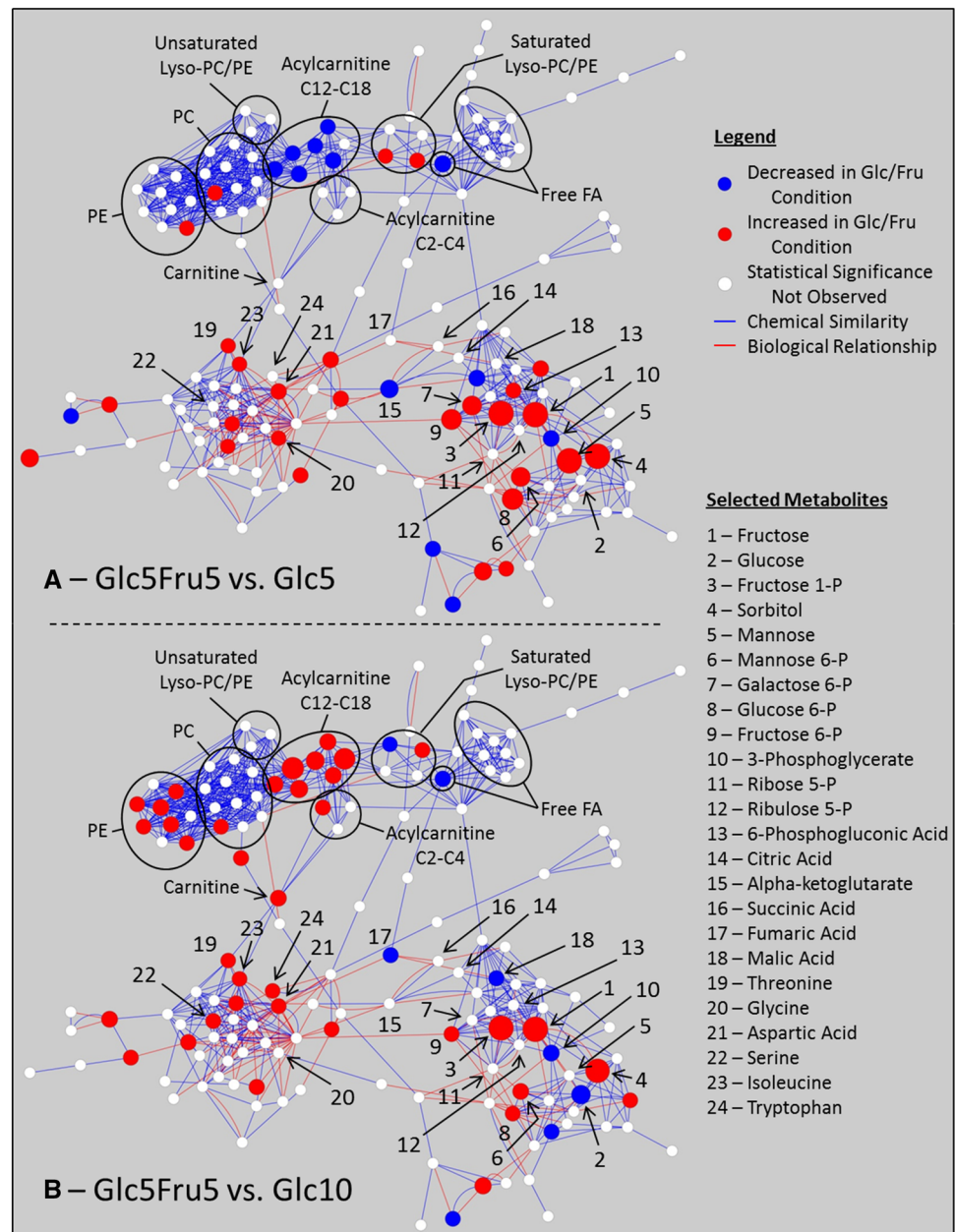
Multivariate clustering by PLS does not readily discern statistical significance of the effects of different carbohydrate loads on HepG2 cells, including directional fold changes and biochemical relationships across the various metabolites. To this end, the MetaMapp software tool was chosen to facilitate interpretation (Barupal et al. 2012). MetaMapp enabled the construction of metabolite networks based on all annotated metabolites (Supplementary Figure S2) in addition to directionality and magnitude of statistically different changes in individual metabolites with respect to carbohydrate loads (Fig. 2). The 1 h time point was selected as a representative time point for metabolite network comparison due to similarity with the 10 min and 6 h results and clear separation of hexose conditions in the PLS analysis. In contrast to multivariate PLS clustering or biochemical MetaMapp network analyses, classic univariate statistics enables more focused interpretations, including the investigation of temporal responses (Table 1 and Fig. 3). In the following, we discuss important metabolic changes for individual metabolic modules.

Fig. 2 Metabolite network analysis of the metabolic response to high-fructose media in HepG2 Cells. The network connects metabolite nodes if metabolite pairs are either found as enzymatic transformations in the KEGG Rpair database, or if metabolites share high chemical similarity using the PubChem substructure fingerprint Tanimoto scores. For further details, see the method section and the method reference (Barupal et al. 2012).

a Comparison of Glc5Fru5 and Glc5 media conditions.

b Comparison of Glc5Fru5 and Glc10 media conditions. *Red nodes* represent metabolites with increased signal intensity in the Glc5Fru5 condition; *blue nodes* represent metabolites with decreased signal intensity in the Glc5Fru5 condition.

White nodes represent metabolites without statistically significant changes. Node sizes scale with magnitude of fold changes. *Blue lines* connect metabolites displaying chemical similarity and red lines connect metabolites related by a known biological reaction. Clusters of metabolites are formed by the total number of biochemical and chemical relationships. Lengths of individual edges do not convey further information. Refer to Supplementary Fig. 2 for a detailed map of all metabolite annotations (Color figure online)



3.2 Detected carbohydrate structures yield results consistent with experimental design

The Glc5Fru5 condition was compared to Glc5 and Glc10 conditions with MetaMapp metabolite networks to identify metabolic changes caused by fructose addition to cell culture media (Fig. 2a,b). Glc5Fru5 comparison to both Glc5 and Glc10 conditions was essential to identify effects caused by fructose due to the substantial difference in total hexose conditions. While the Glc5 condition is representative of physiological blood glucose levels (Daly et al. 1998), observed metabolic differences relative to the Glc5Fru5 condition could be an effect of either fructose

exposure or excess hexose resources. Incorporation of a second MetaMapp metabolite network comparing Glc5Fru5 and Glc10 conditions in the data analysis (Fig. 2b) enabled distinction of metabolic effects caused by fructose per se and not simply excess hexose.

The Glc5Fru5 versus Glc5 MetaMapp metabolite network revealed that in the Glc5Fru5 condition there was substantially elevated levels of cellular fructose, fructose-1-phosphate, sorbitol, mannose, mannose-6-phosphate, and galactose-6-phosphate. The Glc5Fru5 versus Glc10 MetaMapp metabolite network also revealed substantially elevated levels of fructose, fructose-1-phosphate, and sorbitol in the Glc5Fru5 condition, indicating that fructose

Table 1 Fold-changes and *p*-values of selected metabolites in HepG2 cells grown under high carbohydrate or high fructose-containing carbohydrate loads. For a list of all metabolites, see Supplementary Table S1. Grey labels indicate statistical significance (*p* < 0.05). All *p*-values are rounded up to the second decimal

| | metabolite ratios for (glucose + fructose)/(glucose 5 mM) with (<i>p</i> -values) blue if <i>p</i> < 0.05 | | | | Metabolite ratios for (glucose + fructose)/(glucose 10 mM) with (<i>p</i> -values) blue if <i>p</i> < 0.05 | | | |
|-----------------------|--|-------------------------|-------------------------|-------------------------|---|-------------------------|-------------------------|------------------------|
| | 10 min | 1 h | 6 h | 24 h | 10 min | 1 h | 6 h | 24 h |
| fructose | 16.2 (<i>p</i> < 0.04) | 26.6 (<i>p</i> < 0.01) | 23.6 (<i>p</i> < 0.01) | 25.4 (<i>p</i> < 0.06) | 23.2 (<i>p</i> < 0.03) | 14.4 (<i>p</i> < 0.01) | 33.9 (<i>p</i> < 0.01) | 9.8 (<i>p</i> < 0.09) |
| glucose | 0.63 (<i>p</i> < 0.42) | 1.4 (<i>p</i> < 0.17) | 1.3 (<i>p</i> < 0.75) | 1.4 (<i>p</i> < 0.79) | 0.6 (<i>p</i> < 0.46) | 0.5 (<i>p</i> < 0.04) | 0.8 (<i>p</i> < 0.67) | 0.2 (<i>p</i> < 0.22) |
| mannose | 1.0 (<i>p</i> < 1.00) | 6.9 (<i>p</i> < 0.01) | 7.5 (<i>p</i> < 0.01) | 5.5 (<i>p</i> < 0.21) | 1. (<i>p</i> < 0.45) | 1.3 (<i>p</i> < 0.63) | 3.3 (<i>p</i> < 0.07) | 0.7 (<i>p</i> < 0.81) |
| sorbitol | 3.3 (<i>p</i> < 0.01) | 5.0 (<i>p</i> < 0.01) | 5.3 (<i>p</i> < 0.01) | 7.6 (<i>p</i> < 0.01) | 3.8 (<i>p</i> < 0.01) | 3.7 (<i>p</i> < 0.01) | 5.0 (<i>p</i> < 0.01) | 3.0 (<i>p</i> < 0.01) |
| fructose-1-phosphate | 7.2 (<i>p</i> < 0.01) | 5.3 (<i>p</i> < 0.01) | 4.4 (<i>p</i> < 0.01) | 31.2 (<i>p</i> < 0.01) | 3.6 (<i>p</i> < 0.01) | 3.9 (<i>p</i> < 0.01) | 4.6 (<i>p</i> < 0.01) | 7.1 (<i>p</i> < 0.01) |
| galactose-6-phosphate | 0.7 (<i>p</i> < 0.01) | 2.4 (<i>p</i> < 0.01) | 2.3 (<i>p</i> < 0.01) | 4.5 (<i>p</i> < 0.01) | 0.7 (<i>p</i> < 0.03) | 1.1 (<i>p</i> < 0.43) | 0.9 (<i>p</i> < 0.58) | 1.1 (<i>p</i> < 0.55) |
| mannose-6-phosphate | 1.0 (<i>p</i> < 0.94) | 2.3 (<i>p</i> < 0.01) | 2.3 (<i>p</i> < 0.01) | 5.1 (<i>p</i> < 0.01) | 1.1 (<i>p</i> < 0.61) | 1.5 (<i>p</i> < 0.01) | 1.3 (<i>p</i> < 0.05) | 0.9 (<i>p</i> < 0.27) |
| 3-phosphoglycerate | 1.0 (<i>p</i> < 0.96) | 0.7 (<i>p</i> < 0.01) | 0.8 (<i>p</i> < 0.01) | 0.7 (<i>p</i> < 0.01) | 1.0 (<i>p</i> < 0.95) | 0.7 (<i>p</i> < 0.01) | 0.7 (<i>p</i> < 0.01) | 0.5 (<i>p</i> < 0.01) |
| fructose-6-phosphate | 0.7 (<i>p</i> < 0.01) | 2.7 (<i>p</i> < 0.01) | 2.5 (<i>p</i> < 0.01) | 11.7 (<i>p</i> < 0.02) | 0.7 (<i>p</i> < 0.04) | 1.2 (<i>p</i> < 0.04) | 1.3 (<i>p</i> < 0.16) | 2.4 (<i>p</i> < 0.13) |
| glucose-6-phosphate | 0.7 (<i>p</i> < 0.01) | 2.9 (<i>p</i> < 0.01) | 2.6 (<i>p</i> < 0.01) | 6.5 (<i>p</i> < 0.01) | 0.8 (<i>p</i> < 0.06) | 1.2 (<i>p</i> < 0.05) | 1.0 (<i>p</i> < 0.99) | 1.0 (<i>p</i> < 0.91) |
| phosphogluconic acid | 0.7 (<i>p</i> < 0.02) | 1.3 (<i>p</i> < 0.01) | 1.0 (<i>p</i> < 0.65) | 1.4 (<i>p</i> < 0.03) | 0.8 (<i>p</i> < 0.11) | 0.9 (<i>p</i> < 0.17) | 1.0 (<i>p</i> < 0.86) | 0.7 (<i>p</i> < 0.03) |
| ribose-5-phosphate | 1.2 (<i>p</i> < 0.27) | 1.2 (<i>p</i> < 0.17) | 1.0 (<i>p</i> < 0.86) | 1.5 (<i>p</i> < 0.07) | 0.9 (<i>p</i> < 0.65) | 0.9 (<i>p</i> < 0.15) | 0.9 (<i>p</i> < 0.62) | 0.7 (<i>p</i> < 0.05) |
| ribulose-5-phosphate | 1.2 (<i>p</i> < 0.28) | 1.2 (<i>p</i> < 0.29) | 1.1 (<i>p</i> < 0.55) | 1.2 (<i>p</i> < 0.05) | 1.0 (<i>p</i> < 0.73) | 1.1 (<i>p</i> < 0.77) | 1.3 (<i>p</i> < 0.12) | 0.7 (<i>p</i> < 0.03) |
| α-ketoglutaric acid | 1.4 (<i>p</i> < 0.13) | 0.5 (<i>p</i> < 0.04) | 0.6 (<i>p</i> < 0.01) | 1.3 (<i>p</i> < 0.23) | 0.9 (<i>p</i> < 0.07) | 0.6 (<i>p</i> < 0.29) | 0.7 (<i>p</i> < 0.22) | 0.8 (<i>p</i> < 0.10) |
| citric acid | 1.2 (<i>p</i> < 0.04) | 1.0 (<i>p</i> < 0.53) | 0.8 (<i>p</i> < 0.01) | 2.2 (<i>p</i> < 0.01) | 0.7 (<i>p</i> < 0.03) | 0.7 (<i>p</i> < 0.18) | 0.8 (<i>p</i> < 0.01) | 1.1 (<i>p</i> < 0.25) |
| fumaric acid | 1.2 (<i>p</i> < 0.19) | 1.1 (<i>p</i> < 0.26) | 0.9 (<i>p</i> < 0.31) | 1.4 (<i>p</i> < 0.01) | 0.7 (<i>p</i> < 0.02) | 0.8 (<i>p</i> < 0.01) | 1.0 (<i>p</i> < 0.97) | 0.9 (<i>p</i> < 0.17) |
| malic acid | 1.2 (<i>p</i> < 0.10) | 1.0 (<i>p</i> < 0.46) | 0.8 (<i>p</i> < 0.01) | 1.2 (<i>p</i> < 0.02) | 0.6 (<i>p</i> < 0.01) | 0.8 (<i>p</i> < 0.03) | 1.0 (<i>p</i> < 0.85) | 0.9 (<i>p</i> < 0.12) |
| succinic acid | 1.5 (<i>p</i> < 0.09) | 1.2 (<i>p</i> < 0.60) | 0.9 (<i>p</i> < 0.73) | 1.4 (<i>p</i> < 0.40) | 2.1 (<i>p</i> < 0.01) | 1.0 (<i>p</i> < 0.94) | 1.3 (<i>p</i> < 0.26) | 1.1 (<i>p</i> < 0.81) |
| aspartic acid | 1.1 (<i>p</i> < 0.28) | 1.4 (<i>p</i> < 0.01) | 1.4 (<i>p</i> < 0.01) | 1.2 (<i>p</i> < 0.01) | 0.7 (<i>p</i> < 0.06) | 1.2 (<i>p</i> < 0.01) | 1.6 (<i>p</i> < 0.01) | 1.1 (<i>p</i> < 0.13) |
| glycine | 1.3 (<i>p</i> < 0.01) | 1.1 (<i>p</i> < 0.01) | 1.2 (<i>p</i> < 0.01) | 1.3 (<i>p</i> < 0.01) | 1.2 (<i>p</i> < 0.03) | 1.0 (<i>p</i> < 0.74) | 1.3 (<i>p</i> < 0.01) | 1.3 (<i>p</i> < 0.01) |
| isoleucine | 1.1 (<i>p</i> < 0.22) | 1.1 (<i>p</i> < 0.01) | 1.2 (<i>p</i> < 0.02) | 1.2 (<i>p</i> < 0.07) | 1.1 (<i>p</i> < 0.01) | 1.1 (<i>p</i> < 0.01) | 1.2 (<i>p</i> < 0.01) | 1.0 (<i>p</i> < 0.85) |
| serine | 1.2 (<i>p</i> < 0.01) | 1.0 (<i>p</i> < 0.13) | 1.2 (<i>p</i> < 0.05) | 1.7 (<i>p</i> < 0.01) | 1.1 (<i>p</i> < 0.04) | 1.2 (<i>p</i> < 0.01) | 1.6 (<i>p</i> < 0.01) | 1.9 (<i>p</i> < 0.01) |
| threonine | 1.2 (<i>p</i> < 0.01) | 1.1 (<i>p</i> < 0.01) | 1.2 (<i>p</i> < 0.01) | 1.4 (<i>p</i> < 0.01) | 1.1 (<i>p</i> < 0.01) | 1.1 (<i>p</i> < 0.01) | 1.3 (<i>p</i> < 0.01) | 1.1 (<i>p</i> < 0.01) |
| tryptophan | 1.1 (<i>p</i> < 0.07) | 1.1 (<i>p</i> < 0.27) | 1.2 (<i>p</i> < 0.04) | 1.1 (<i>p</i> < 0.21) | 1.2 (<i>p</i> < 0.01) | 1.1 (<i>p</i> < 0.02) | 1.3 (<i>p</i> < 0.01) | 1.0 (<i>p</i> < 0.84) |
| carnitine | 0.9 (<i>p</i> < 0.10) | 1.1 (<i>p</i> < 0.70) | 0.7 (<i>p</i> < 0.01) | 1.7 (<i>p</i> < 0.01) | 1.2 (<i>p</i> < 0.11) | 1.5 (<i>p</i> < 0.01) | 0.9 (<i>p</i> < 0.46) | 1.1 (<i>p</i> < 0.46) |
| acylcarnitine C2:0 | 1.1 (<i>p</i> < 0.59) | 1.0 (<i>p</i> < 0.96) | 1.0 (<i>p</i> < 0.70) | 1.1 (<i>p</i> < 0.62) | 0.8 (<i>p</i> < 0.06) | 1.0 (<i>p</i> < 0.94) | 0.9 (<i>p</i> < 0.70) | 1.3 (<i>p</i> < 0.03) |
| acylcarnitine C3:0 | 0.9 (<i>p</i> < 0.22) | 1.2 (<i>p</i> < 0.09) | 1.1 (<i>p</i> < 0.38) | 1.3 (<i>p</i> < 0.05) | 1.1 (<i>p</i> < 0.24) | 1.3 (<i>p</i> < 0.05) | 1.0 (<i>p</i> < 0.92) | 1.0 (<i>p</i> < 0.74) |
| acylcarnitine C4:0 | 1.0 (<i>p</i> < 0.96) | 1.1 (<i>p</i> < 0.69) | 0.8 (<i>p</i> < 0.10) | 2.1 (<i>p</i> < 0.01) | 1.1 (<i>p</i> < 0.39) | 1.7 (<i>p</i> < 0.11) | 1.0 (<i>p</i> < 0.74) | 1.2 (<i>p</i> < 0.09) |
| acylcarnitine C12:0 | 0.9 (<i>p</i> < 0.17) | 1.0 (<i>p</i> < 0.76) | 1.6 (<i>p</i> < 0.02) | 0.8 (<i>p</i> < 0.07) | 2.1 (<i>p</i> < 0.01) | 2.9 (<i>p</i> < 0.01) | 2.3 (<i>p</i> < 0.01) | 3.5 (<i>p</i> < 0.01) |
| acylcarnitine C14:0 | 0.7 (<i>p</i> < 0.01) | 0.8 (<i>p</i> < 0.01) | 1.4 (<i>p</i> < 0.03) | 0.6 (<i>p</i> < 0.01) | 1.8 (<i>p</i> < 0.01) | 2.1 (<i>p</i> < 0.01) | 1.6 (<i>p</i> < 0.01) | 3.0 (<i>p</i> < 0.01) |
| acylcarnitine C14:1 | 0.6 (<i>p</i> < 0.01) | 0.8 (<i>p</i> < 0.02) | 1.4 (<i>p</i> < 0.05) | 0.5 (<i>p</i> < 0.01) | 2.3 (<i>p</i> < 0.01) | 3.1 (<i>p</i> < 0.01) | 2.2 (<i>p</i> < 0.01) | 3.4 (<i>p</i> < 0.01) |
| acylcarnitine C16:0 | 0.8 (<i>p</i> < 0.01) | 0.8 (<i>p</i> < 0.01) | 1.4 (<i>p</i> < 0.02) | 0.6 (<i>p</i> < 0.01) | 1.4 (<i>p</i> < 0.01) | 1.6 (<i>p</i> < 0.01) | 1.4 (<i>p</i> < 0.03) | 2.6 (<i>p</i> < 0.01) |
| acylcarnitine C16:1 | 0.5 (<i>p</i> < 0.01) | 0.7 (<i>p</i> < 0.01) | 1.5 (<i>p</i> < 0.02) | 0.6 (<i>p</i> < 0.01) | 1.4 (<i>p</i> < 0.01) | 1.9 (<i>p</i> < 0.01) | 1.6 (<i>p</i> < 0.01) | 2.8 (<i>p</i> < 0.01) |

Table 1 continued

| | metabolite ratios for (glucose + fructose)/(glucose 5 mM) with (<i>p</i> -values) blue if <i>p</i> < 0.05 | | | | Metabolite ratios for (glucose + fructose)/(glucose 10 mM) with (<i>p</i> -values) blue if <i>p</i> < 0.05 | | | |
|-----------------------|--|------------------------|------------------------|------------------------|---|------------------------|------------------------|-------------------------|
| | 10 min | 1 h | 6 h | 24 h | 10 min | 1 h | 6 h | 24 h |
| acetylcarbitine C18:0 | 0.7 (<i>p</i> < 0.01) | 0.7 (<i>p</i> < 0.01) | 1.4 (<i>p</i> < 0.05) | 0.6 (<i>p</i> < 0.01) | 1.6 (<i>p</i> < 0.01) | 1.6 (<i>p</i> < 0.01) | 1.4 (<i>p</i> < 0.08) | 2.6 (<i>p</i> < 0.01) |
| acetylcarbitine C18:1 | 0.6 (<i>p</i> < 0.01) | 0.7 (<i>p</i> < 0.01) | 1.5 (<i>p</i> < 0.01) | 0.6 (<i>p</i> < 0.01) | 1.3 (<i>p</i> < 0.04) | 1.6 (<i>p</i> < 0.01) | 1.5 (<i>p</i> < 0.02) | 2.3 (<i>p</i> < 0.010) |
| oleic acid | 0.8 (<i>p</i> < 0.37) | 0.6 (<i>p</i> < 0.01) | 2.4 (<i>p</i> < 0.29) | 1.3 (<i>p</i> < 0.10) | 1.2 (<i>p</i> < 0.59) | 0.7 (<i>p</i> < 0.01) | 3.0 (<i>p</i> < 0.24) | 1.2 (<i>p</i> < 0.14) |
| lysoPC 16:0 | 1.0 (<i>p</i> < 0.42) | 1.1 (<i>p</i> < 0.04) | 0.9 (<i>p</i> < 0.14) | 1.2 (<i>p</i> < 0.04) | 0.8 (<i>p</i> < 0.01) | 0.9 (<i>p</i> < 0.09) | 0.8 (<i>p</i> < 0.01) | 0.8 (<i>p</i> < 0.01) |
| lysoPC 16:1 | 0.8 (<i>p</i> < 0.03) | 1.0 (<i>p</i> < 0.67) | 1.0 (<i>p</i> < 0.53) | 1.2 (<i>p</i> < 0.09) | 0.9 (<i>p</i> < 0.11) | 1.1 (<i>p</i> < 0.28) | 1.0 (<i>p</i> < 0.99) | 1.2 (<i>p</i> < 0.30) |
| lysoPC 18:0 | 0.9 (<i>p</i> < 0.07) | 1.0 (<i>p</i> < 0.96) | 0.9 (<i>p</i> < 0.12) | 1.1 (<i>p</i> < 0.41) | 0.7 (<i>p</i> < 0.01) | 0.9 (<i>p</i> < 0.01) | 0.7 (<i>p</i> < 0.01) | 0.7 (<i>p</i> < 0.01) |
| lysoPC 18:1 | 0.9 (<i>p</i> < 0.21) | 1.1 (<i>p</i> < 0.10) | 1.0 (<i>p</i> < 0.43) | 1.2 (<i>p</i> < 0.03) | 0.8 (<i>p</i> < 0.01) | 0.9 (<i>p</i> < 0.16) | 0.8 (<i>p</i> < 0.02) | 0.8 (<i>p</i> < 0.01) |
| PE 32:1 | 0.8 (<i>p</i> < 0.03) | 1.0 (<i>p</i> < 0.69) | 1.0 (<i>p</i> < 0.27) | 0.9 (<i>p</i> < 0.37) | 1.1 (<i>p</i> < 0.48) | 1.4 (<i>p</i> < 0.01) | 1.3 (<i>p</i> < 0.01) | 1.7 (<i>p</i> < 0.01) |
| PE 32:2 | 0.8 (<i>p</i> < 0.04) | 0.9 (<i>p</i> < 0.17) | 1.0 (<i>p</i> < 0.82) | 0.9 (<i>p</i> < 0.33) | 1.4 (<i>p</i> < 0.01) | 1.6 (<i>p</i> < 0.01) | 1.5 (<i>p</i> < 0.01) | 1.9 (<i>p</i> < 0.01) |
| PE 34:1 | 0.7 (<i>p</i> < 0.01) | 1.0 (<i>p</i> < 0.62) | 1.0 (<i>p</i> < 0.74) | 0.8 (<i>p</i> < 0.03) | 1.0 (<i>p</i> < 0.99) | 1.2 (<i>p</i> < 0.01) | 1.3 (<i>p</i> < 0.01) | 1.4 (<i>p</i> < 0.01) |
| PE 34:2 | 0.8 (<i>p</i> < 0.02) | 1.0 (<i>p</i> < 0.68) | 1.0 (<i>p</i> < 0.48) | 1.0 (<i>p</i> < 0.81) | 1.0 (<i>p</i> < 0.76) | 1.2 (<i>p</i> < 0.01) | 1.3 (<i>p</i> < 0.02) | 1.5 (<i>p</i> < 0.01) |
| PE 36:2 | 0.8 (<i>p</i> < 0.02) | 1.1 (<i>p</i> < 0.16) | 1.0 (<i>p</i> < 0.93) | 1.0 (<i>p</i> < 0.86) | 0.9 (<i>p</i> < 0.44) | 1.1 (<i>p</i> < 0.07) | 1.2 (<i>p</i> < 0.01) | 1.3 (<i>p</i> < 0.02) |
| PE 36:4 | 0.8 (<i>p</i> < 0.06) | 1.1 (<i>p</i> < 0.35) | 1.0 (<i>p</i> < 1.00) | 1.1 (<i>p</i> < 0.39) | 0.9 (<i>p</i> < 0.36) | 1.1 (<i>p</i> < 0.15) | 1.2 (<i>p</i> < 0.03) | 1.3 (<i>p</i> < 0.06) |
| PE 38:6 | 0.8 (<i>p</i> < 0.08) | 1.1 (<i>p</i> < 0.09) | 1.1 (<i>p</i> < 0.22) | 1.2 (<i>p</i> < 0.03) | 0.93 (<i>p</i> < 0.47) | 1.1 (<i>p</i> < 0.11) | 1.3 (<i>p</i> < 0.01) | 1.4 (<i>p</i> < 0.01) |

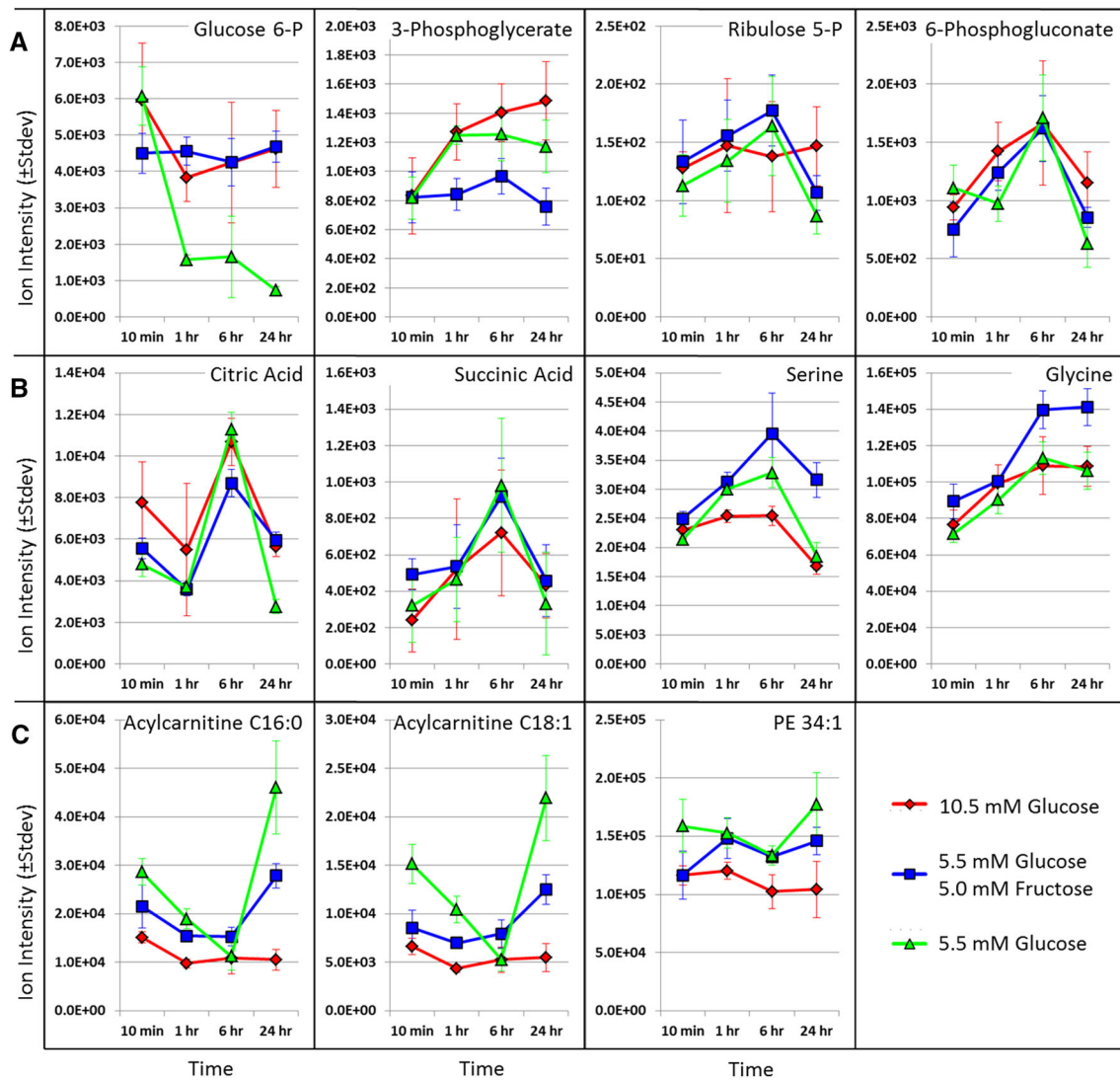


Fig. 3 Temporal responses of selected metabolites to different carbohydrate growth media in HepG2 Cells. **a** glycolysis and pentose phosphate pathway metabolites. **b** tricarboxylic acid cycle metabolites. **c** long-chain acylcarnitines

exposure led to an increased abundance of these particular metabolites, as expected. In comparison, mannose and galactose-6-phosphate did not display statistically significant variation between Glc5Fru5 and Glc10 experimental conditions, suggesting a generic effect of high total hexose concentrations on generation of these metabolites. While mannose-6-phosphate levels were elevated in the Glc5Fru5 condition versus Glc10 comparison, the fold change was relatively small compared to the fold change observed in the Glc5Fru5 versus Glc5 comparison, implicating again that such metabolic conversions appear to be dependent on overall high hexose concentrations. These six metabolites were subject to a more detailed comparison at all sampling time points to facilitate a better understanding of the fructose and hexose concentration-dependent effects (Table 1).

Consistent with the experimental design, fructose levels were elevated in the Glc5Fru5 condition at all sampling time points in both Glc5Fru5 versus Glc5 and Glc5Fru5 versus Glc10 comparisons. In addition, fructose-1-phosphate and sorbitol levels were elevated in the Glc5Fru5 condition at all sampling time points in both comparisons. This result supports the validity of the experimental model, because fructose-1-phosphate and sorbitol are formed directly from fructose via known enzymatic reactions in liver tissues. Fructokinase phosphorylates fructose to form fructose-1-phosphate (Heinz et al. 1968; Mayes 1993), and sorbitol dehydrogenase catalyzes reduction of fructose, yielding sorbitol (Blakley 1951; Maret and Auld 1987). Comparison of Glc5Fru5 and Glc5 data sets revealed two- to eight-fold elevated levels of mannose, mannose-6-phosphate, and galactose-6-phosphate metabolites in the

Glc5Fru5 condition at all sampling time points after 10 min. The same trend was not observed in the comparison of Glc5Fru5 and Glc10 conditions: mannose-6-phosphate levels were elevated by only 40 % in the Glc5Fru5 condition at 1 and 6 h and did not display statistically significant differences at 10 min or 24 h sampling time points, and mannose and galactose-6-phosphate did not display a statistically significant differences at any time point. This temporal result analysis confirms that the differences observed in mannose, mannose-6-phosphate, and galactose-6-phosphate levels in comparison of Glc5Fru5 and Glc5 data sets are predominantly due to a difference in total hexose resources.

3.3 High fructose load elicits a decrease in cellular levels of the glycolytic intermediate 3-phosphoglycerate

The metabolomic data sets contained several intermediates of the glycolysis pathway, including glucose-6-phosphate, fructose-6-phosphate, and 3-phosphoglycerate as well as several metabolites from the pentose phosphate pathway (PPP) such as ribose-5-phosphate, ribulose-5-phosphate, and 6-phosphogluconic acid. The MetaMapp metabolite networks at 1 h post-treatment indicated several statistically significant differences in these six metabolites. The Glc5Fru5 versus Glc5 metabolite network revealed elevated levels of glucose-6-phosphate, fructose 6-phosphate, and 6-phosphogluconic acid as well as decreased levels of 3-phosphoglycerate in the Glc5Fru5 condition (Fig. 2a). The Glc5Fru5 versus Glc10 metabolite network indicated similar trends in the three glycolysis metabolites, although the fold-changes for glucose-6-phosphate and fructose-6-phosphate were substantially lower than observed in the Glc5Fru5 versus Glc5 metabolite network. Statistically significant differences were not observed in PPP metabolites in the 1 h Glc5Fru5 versus Glc10 metabolite network, indicating that changes in the PPP relative to the Glc5 condition were a result of excess hexoses and not fructose per se.

To better understand the relationship of sampling time and metabolite abundance, several metabolites of the glycolysis and PPP pathways were graphed according to their sampling times (Fig. 3a). The time-based analysis indicates that glucose-6-phosphate levels were relatively maintained in the Glc5Fru5 and Glc10 conditions while abundance dropped after 10 min in the Glc5 condition, as we previously reported (Hirahatake et al. 2011). This result indicates that total hexose levels can drastically alter metabolite levels at early stages of glycolysis and for long periods thereafter. 3-phosphoglycerate levels were also relatively similar between Glc5Fru5, Glc5, and Glc10 experimental conditions at 10 min, but

3-phosphoglycerate levels increased at later time points for both glucose conditions. 3-phosphoglycerate levels were 30 % lower in the Glc5Fru5 data set compared to the Glc5 data set from 1 to 24 h time points (Table 1). Comparison of Glc5Fru5 and Glc10 data sets yielded a similar result, indicating that increases in 3-phosphoglycerate levels in the HepG2 model system are specific to glucose. Statistically significant differences spanning multiple time points were not observed for either ribose-5-phosphate or ribulose-5-phosphate in comparison of Glc5Fru5, Glc5, and Glc10 data sets. 6-phosphogluconic acid did not present statistically significant differences at multiple time points in comparison of Glc5Fru5 and Glc10 data sets, but differences were observed in comparison of Glc5Fru5 and Glc5 data sets. However, fold change directionality was extremely erratic for 6-phosphogluconic acid in the Glc5Fru5 versus Glc5 comparison and a clear trend spanning multiple time points could not be identified.

The observed decrease in 3-phosphoglycerate levels in the Glc5Fru5 condition, despite substantially elevated amounts of fructose-1-phosphate, was a particularly interesting result. This was not anticipated because increased 3-phosphoglycerate levels, although much smaller in magnitude and concentration relative to fructose-1-phosphate levels, have been reported with a rat liver hepatocyte model system treated with an estimated 12 mM fructose (Grivell et al. 1991). In addition, fructose metabolism involves conversion of fructose to triose phosphates which enter glycolysis downstream of phosphofructokinase-mediated regulatory mechanisms (Havel 2005; Hirahatake et al. 2011; Mayes 1993) and thus should serve as ready sources of 3-phosphoglycerate precursor. This characteristic of hepatic fructose metabolism has led to the proposal that the hyperlipidemic phenotype seen after high fructose feeding is a consequence of increased availability of glycolysis metabolites that feed into fatty acid biosynthesis (Mayes 1993). Perhaps biochemical regulation exists in HepG2 cells to mediate the conversion of fructose-1-phosphate-derived triose phosphates into 3-phosphoglycerate. Several enzymes catalyze the conversion of fructose-1-phosphate to 3-phosphoglycerate including aldolase B, triokinase, triosephosphate isomerase, glyceraldehyde phosphate dehydrogenase, and phosphoglycerate kinase (Heinz et al. 1968; Mayes 1993). Regulation of activity or expression of one or more of these enzymes following fructose exposure could potentially explain the experimental results presented here. It is also acknowledged that it is not yet known if outcomes in response to fructose in the HepG2 hepatoma cell line fully reflect 3-phosphoglycerate and triose phosphate flux in human liver in vivo upon fructose ingestion.

3.4 Tricarboxylic acid cycle metabolites display a clear temporal regulation

Identified intermediates of the tricarboxylic acid (TCA) cycle included alpha-ketoglutarate, citric acid, fumaric acid, malic acid, and succinic acid. MetaMapp metabolite networks from the 1 h treatment time point did not reveal many substantial differences in TCA cycle metabolites across treatments. Glc5Fru5 media yielded lower levels of alpha-ketoglutarate in comparison to the Glc5 condition (Fig. 2a). Similarly, in the Glc5Fru5 condition lower levels of fumaric and malic acid were observed in comparison to Glc10 media (Fig. 2b). Although other TCA intermediates were unaffected, as demonstrated in the corresponding MetaMapp networks, two TCA cycle metabolites were graphed according to sampling time plots due to the crucial role of the TCA cycle in energy metabolism (Fig. 3b).

Considering the importance of TCA cycle intermediate dynamics in oxidative hexose metabolism and lipogenesis, TCA cycle metabolites were graphed according to sampling time (Fig. 3b). Citrate levels decreased between 10 min and 1 h after exchanging culture media, substantially rising until the 6 h time point, and dropping at the 24 h time point for all hexose conditions. While all culture media followed the same time-dependent trend for citrate levels, the Glc5 condition displayed the highest variability over time as it displayed the greatest increase between 1 and 6 h after exchanging culture media, concomitant with the greatest decrease between 6 and 24 h time points of all tested hexose conditions. This same general trend was observed for the other TCA cycle metabolites. Similar to citrate, the Glc5 condition presented the greatest increase for the all TCA cycle metabolites between 1 and 6 h after exchanging to fresh hexose media, and the greatest decrease between the 6 and 24 h time points. These time-dependent changes of the TCA cycle metabolites are a particularly notable effect in the metabolomics data set, and similar temporal changes for TCA cycle compounds are observed in acetate-grown *Chlamydomonas reinhardtii* cultures (Lee et al. 2012), indicating more fundamental relationships of cellular regulation that are independent of the amount or type of carbon source. It is important to note that these coordinated and large temporal changes were observed despite substantial efforts to maintain static physiological conditions throughout the experimental design. HepG2 cells were incubated in media representative of each experimental condition for 48 h with daily media changes prior to harvesting cells. This approach acclimated HepG2 cells toward their respective experimental conditions to obtain a metabolite profile representative of continued exposure instead of response to a sudden change in carbohydrate resources. Nevertheless, media replacements provided a boost in substrate

concentration compared to that left over from the prior 24 h culture, which in turn clearly elicited dynamic shifts in cellular metabolite profiles..

3.5 High fructose media causes an increase in cellular glycine, threonine, and serine pools

Untargeted metabolomics enabled quantitative assessments of 18 different free amino acids. Five of these amino acids were found to be differentially regulated comparing Glc5Fru5 to Glc5 media (Fig. 2a), and seven amino acids were found at statistically different levels in Glc5Fru5 compared to Glc10 conditions (Fig. 2b). Similar to TCA intermediates, these amino acid pools were subject to temporal analyses. Significantly elevated levels of threonine, glycine and serine were found for the high fructose media in comparison to either high-glucose and standard Glc5 media at three or more time points (Table 1). In addition, the Glc5Fru5 treatment also increased levels of isoleucine and tryptophan in comparison to Glc10 conditions at three or more sampling time points. These results suggest that fructose is a specific factor causing elevated levels of several amino acids in HepG2 cells. The greater abundance of serine in the Glc5Fru5 condition is a particularly noteworthy result because 3-phosphoglycerate is a biosynthetic precursor of glycine and serine amino acids (Umberger 1978). Reduced levels of 3-phosphoglycerate as substrate in coordination with higher levels of its amino acid products indicates that some carbon flux may be redirected toward amino acid biosynthesis under high fructose conditions. Interestingly, glycine and serine are two amino acids that are directly involved in one-carbon transfer between cytoplasmic and mitochondrial folate pathways (Appling 1991; Tibbetts and Appling 2010), suggesting fructose may also influence one-carbon metabolism. Elevated levels of threonine is also an interesting result as, though a minor pathway in threonine catabolism, threonine may potentially enter one-carbon metabolic pathways via conversion to glycine (Darling et al. 2000; Locasale 2013). Reviews on isotope-labeled fructose metabolism failed to detail changes in amino acid metabolism (Sun and Empie 2012) which we found here to be an important off-site effect from glycolytic 3-phosphoglycerate in the study presented here, indicating the complementary nature of targeted and untargeted metabolomics studies. A metabolome study in 377 Framingham cohort subjects on the effects of oral glucose tolerance testing confirmed our finding of dysregulation of amino acid metabolism under high carbohydrate loads, and also did not see immediate changes in triglyceride contents (Ho et al., 2013). However, other studies showed that de-novo lipogenesis is increased from 5 to 26 % under high fructose diets (Basaranoglu et al. 2013), linking fructose

metabolism directly to the development of nonalcoholic fatty liver disease in humans.

3.6 High carbohydrate loads affect levels of long-chain acylcarnitines

The MetaMapp metabolite networks revealed a clear impact of hexoses on acylcarnitine levels. The Glc5Fru5 versus Glc5 metabolite network indicated that six of seven detected acylcarnitines with acyl chain lengths between 12 and 18 carbons were lowered under high-fructose media conditions relative the Glc5 condition (Fig. 2a). This result may be anticipated as fructose decreases hepatic fatty acid oxidation (Topping and Mayes 1972) likely through the accumulation of the carnitine palmitoyltransferase 1 inhibitor malonyl-CoA (not measured here) (Roglans et al. 2002; Vilà et al. 2011). Interestingly, the Glc5Fru5 versus Glc10 metabolite network revealed significantly higher levels of long chain acylcarnitine levels under high-fructose conditions in comparison to an equally high hexose load composed only of glucose (Fig. 2b). This may indicate that excess glucose causes an even greater accumulation of malonyl-CoA compared to a glucose/fructose mixture of equal concentration. When analyzing the temporal changes of acylcarnitine levels (Fig. 3c), opposite trends to the regulation of TCA metabolites (Fig. 3b) were observed for the standard Glc5 condition, with acylcarnitines dropping between 10 min and 6 h post-change in culture media and similar patterns for the high-glucose Glc10 condition. Similarly to the changes in TCA metabolites, metabolic differences for acylcarnitines were largest within the standard Glc5 condition compared to high-hexose load media, and for most time points, also absolute levels of acylcarnitines were highest in Glc5 media, indicating that excess hexose lowers long chain acylcarnitine levels. The inverse relation of acylcarnitine levels and TCA cycle intermediates indicate different levels of overall mitochondrial respiration activity. Total acylcarnitine levels are an indicator of lipid oxidation activity, which was highest at the 24 h after culture media exchange, at which point the activity of the TCA cycle was lowest.

The acylcarnitine results suggest that high hexose load, either as a glucose/fructose mixture or glucose alone, reduce CPT-1 activity, likely due to accumulation of malonyl-CoA. These results do not support the hypothesis that the specific fructose structure, by bypassing the major regulatory point of glycolysis, leads to increased availability of acetyl-CoA as lipid biosynthetic precursor via carboxylation to malonyl-CoA (Wakil et al. 1983). Malonyl-CoA acts as inhibitor of carnitine palmitoyltransferase 1 which catalyzes the formation of acylcarnitine structures

and is the major regulatory point of fatty acid oxidation (McGarry and Brown 1997; McGarry and Foster 1980). Consistent with previous findings (Roglans et al. 2002; Topping and Mayes 1972; Vilà et al. 2011), comparison of Glc5Fru5 and Glc5 experimental conditions revealed lower levels of long chain acylcarnitines in the high-fructose condition. However, the excess glucose Glc10 media caused an even greater reduction in acylcarnitine levels than the glucose/fructose mixture. If bypassing the major regulatory point of glycolysis leads to increased availability of lipid biosynthetic precursors promoting lipid biosynthesis, the fructose/glucose mixture should have yielded lower acylcarnitine levels than the excess glucose condition due to the inhibitory effect of malonyl-CoA. Should HepG2 cells reflect human liver lipid metabolism, these results indicate that a flux-driven mechanism bypassing phosphofructokinase might not be responsible for the increased lipid production that is generally associated with hepatic fructose metabolism. Our results rather support the notion that fructose metabolism entails more complex regulatory mechanisms mediating the flow of carbon into various biochemical pathways, including sorbitol and amino acid pools.

3.7 Excess glucose causes a reduction in phosphatidylethanolamines but an increase in lyso-phosphatidylcholines

Several classes of lipid structures were detected in HepG2 cell extracts including free fatty acids, PCs, PEs, Lyso-PCs, and Lyso-PEs. The Glc5Fru5 versus Glc5 metabolite network revealed few changes in any of these structures (Fig. 2a), indicating that fructose had little impact on their abundance. However, the Glc5Fru5 versus Glc10 comparison revealed clear differences spanning most PE and Lyso-PC structures (Fig. 2b). While PE levels were relatively comparable between Glc5Fru5 and Glc10 conditions at 10 min, the Glc10 condition displayed progressively lower relative amounts of PE structures with increasing time post media change (Table 1). This trend spanned all nine annotated PE structures and individual data points typically presented a high degree of statistical significance. The largest differences were also observed in PEs with shorter acyl chain lengths. Comparison of Glc5 and Glc10 (Fig. 4) conditions revealed a similar trend toward progressively lower amounts of PE metabolites in the Glc10 condition with increasing time, and greater fold change magnitude with PEs containing shorter acyl chain length (Supplementary Figure S3).

Similar to PEs, Lyso-PC structures did not display broad class dependent changes in the Glc5Fru5 versus Glc5 comparison. However, comparison of Glc5Fru5 and Glc10 data sets revealed three of four annotated Lyso-PC

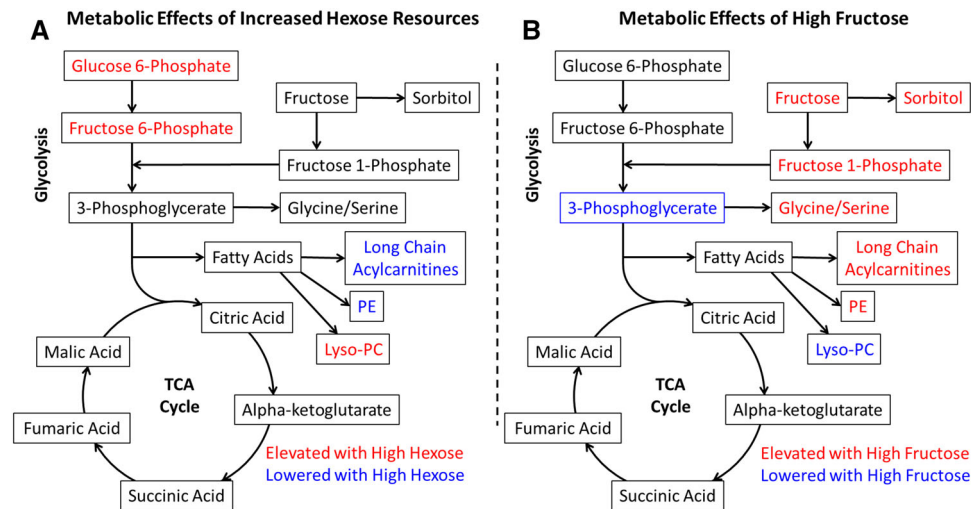


Fig. 4 Changes in HepG2 cell metabolic state due to increased hexose resources and fructose exposure. **a** Metabolic effects of increased hexose resources. *Red labeling* represents metabolites with elevated abundance due to increased hexose resources (10.5 mM glucose vs 5.5 mM glucose media). *Blue labeling* represents metabolites with lowered abundance due to increased hexose resources.

Green labeling represents metabolites with lowered abundance due to only excess glucose. **b** Metabolic effects of high fructose media (10.5 mM glucose vs (5.5 mM glucose + 5.0 mM fructose) media). *Red labeling* represents metabolites with elevated abundance due to fructose exposure. *Blue labeling* represents metabolites with lowered abundance due to fructose exposure (Color figure online)

structures displayed ~24 % elevated levels in the Glc10 condition across all time points (Table 1). Comparison of Glc5 and Glc10 conditions also revealed an average 17 % increase of these three Lyso-PC structures in the Glc10 condition. These results indicate that excess glucose, but not a glucose/fructose mixture, causes reduction of PE and increase in Lyso-PC lipids in HepG2 cells.

A publication applying metabolomics strategies to hepatic tissue collected from a rat model fed a high fructose diet reported significant decreases in several PCs and increases in several Lyso-PC structures relative to controls fed a standard chow diet (Lin et al. 2011). While we did not observe broad statistically significant changes in either PC or Lyso-PC compounds between Glc5Fru5 and Glc5 conditions, we did observe a relative increase in Lyso-PC structures and a decrease in PE structures in the excess glucose condition. PCs and PEs are metabolically linked in the liver by phosphatidylethanolamine N-methyltransferase, which catalyzes methylation of PE, using S-adenosylmethionine as a methyl donor, to form PC (Vance and Ridgway 1988; Vance 2008). Cyclic regeneration of S-adenosylmethionine entails methyl transfer from folate structures (Loenen 2006; Scott 1999). Considering fructose exposure also altered glycine and serine abundance, two amino acids involved in folate metabolism (Appling 1991; Tibbetts and Appling 2010), it is a strong possibility that both the concentration and the type of nutritional carbohydrates have an impact on one-carbon metabolism.

4 Concluding remarks

This metabolomics study provides new insight into the global metabolic effects of fructose metabolism and adds to a more detailed understanding of how fructose impacts metabolism in a cell model of human hepatocyte metabolism. The HepG2 cell line was applied as surrogate for human liver functioning because obtaining liver biopsies from human subjects consuming high glucose or high fructose diets, especially after acute exposure to these hexoses, are impractical due to logistical and ethical considerations. Despite previous validation demonstrating expression of various lipogenic and hexose metabolic genes in these cells (Hirahatake et al. 2011), the HepG2 model system is a hepatoma-derived line studied under conditions lacking the complex hormonal, metabolic and neuronal environment of human liver in situ. Thus, it remains to be seen if the observed changes in metabolite profiles will translate to humans in vivo. Nevertheless, our comprehensive evaluation of 156 identified metabolites and the PLS analysis of unannotated metabolite ions provide first-time evidence for dramatic temporal differences in multi-pathway hepatocyte metabolism based on hexose exposure and type of sugars. Comparative analysis of the effects of different loads of carbohydrates revealed effects on glycolysis, lipid oxidation, amino acid metabolism and complex lipids, with possible implications for one-carbon metabolism as well.

Acknowledgments We thank Wan Tan and Gert Wohlgemuth for their assistance with the GC-TOF platform. Financial support was provided by the National Institutes of Health U24 DK097154 (O.F.), R01 DK078328 (S.H.A., O.F.) and P20 HL113452 (O.F.), the Diabetes Action and Research Education Fund U24 DK097154 (S.H.A.), and USDA-ARS Intramural Projects 51530-016-00D and 5306-51530-019-00 (S.H.A.).

Conflict of interest The authors declare that they have no conflict of interest.

Ethical statement on research This article does not contain any studies with human participants or animals performed by any of the authors.

References

- Appling, D. R. (1991). Compartmentation of folate-mediated one-carbon metabolism in eukaryotes. *FASEB Journal*, 5(12), 5645.
- Barupal, D. K., Haldiya, P. K., Wohlgemuth, G., Kind, T., Kothari, S. L., Pinkerton, K. E., et al. (2012). MetaMapp: mapping and visualizing metabolomic data by integrating information from biochemical pathways and chemical and mass spectral similarity. *BMC Bioinformatics*, 13, 99.
- Basaranoglu, M., Basaranoglu, G., Sabuncu, T., & Sentürk, H. (2013). Fructose as a key player in the development of fatty liver disease. *World Journal of Gastroenterology*, 19(8), 1166.
- Beck-Nielsen, H., Pedersen, O., & Lindskov, H. O. (1980). Impaired cellular insulin binding and insulin sensitivity induced by high-fructose feeding in normal subjects. *The American Journal of Clinical Nutrition*, 33(2), 273–278.
- Blakley, R. L. (1951). The metabolism and antiketogenic effects of sorbitol; sorbitol dehydrogenase. *The Biochemical Journal*, 49(3), 257–271.
- Bray, G. A., Nielsen, S. J., & Popkin, B. M. (2004). Consumption of high-fructose corn syrup in beverages may play a role in the epidemic of obesity. *The American Journal of Clinical Nutrition*, 79(4), 537–543.
- Bruckdorfer, K. R., Khan, I. H., & Yudkin, J. (1972). Fatty acid synthetase activity in the liver and adipose tissue of rats fed with various carbohydrates. *The Biochemical Journal*, 129(2), 439–446.
- Daly, M. E., Vale, C., Walker, M., Alberti, K. G., & Mathers, J. C. (1997). Dietary carbohydrates and insulin sensitivity: a review of the evidence and clinical implications. *The American Journal of Clinical Nutrition*, 66(5), 1072–1085.
- Daly, M. E., Vale, C., Walker, M., Littlefield, A., Alberti, K. G., & Mathers, J. C. (1998). Acute effects on insulin sensitivity and diurnal metabolic profiles of a high-sucrose compared with a high-starch diet. *The American Journal of Clinical Nutrition*, 67(6), 1186–1196.
- Darling, P. B., Grunow, J., Rafii, M., Brookes, S., Ball, R. O., & Pencharz, P. B. (2000). Threonine dehydrogenase is a minor degradative pathway of threonine catabolism in adult humans. *American Journal of Physiology Endocrinology and Metabolism*, 278(5), E877–E884.
- Detmer, K., Aronov, P. A., & Hammock, B. D. (2007). Mass spectrometry-based metabolomics. *Mass Spectrometry Reviews*, 26(1), 51–78.
- Elliott, S. S., Keim, N. L., Stern, J. S., Teff, K., & Havel, P. J. (2002). Fructose, weight gain, and the insulin resistance syndrome. *The American Journal of Clinical Nutrition*, 76(5), 911–922.
- Fiehn, O. (2002). Metabolomics—the link between genotypes and phenotypes. *Plant Molecular Biology*, 48(1–2), 155–171.
- Fiehn, O., Garvey, W. T., Newman, J. W., Lok, K. H., Hoppel, C. L., & Adams, S. H. (2010). Plasma metabolomic profiles reflective of glucose homeostasis in non-diabetic and type 2 diabetic obese African-American women. *PLoS ONE*, 5(12), e15234.
- Fiehn, O., Wohlgemuth, G., & Scholz, M. (2005). Setup and Annotation of Metabolomic Experiments by Integrating Biological and Mass Spectrometric Metadata. *Lecture Notes in Computer Science*, 3615, 224–239.
- Fiehn, O., Wohlgemuth, G., Scholz, M., Kind, T., Lee do, Y., Lu, Y., et al. (2008). Quality control for plant metabolomics: reporting MSI-compliant studies. *The Plant Journal: For Cell and Molecular Biology*, 53(4), 691–704.
- Fried, S. K., & Rao, S. P. (2003). Sugars, hypertriglyceridemia, and cardiovascular disease. *The American Journal of Clinical Nutrition*, 78(4), 873S–880S.
- Grivell, A. R., Halls, H. J., & Berry, M. N. (1991). Role of mitochondria in hepatic fructose metabolism. *Biochimica et Biophysica Acta*, 1059(1), 45–54.
- Hallfrisch, J., Reiser, S., & Prather, E. S. (1983). Blood lipid distribution of hyperinsulinemic men consuming three levels of fructose. *The American Journal of Clinical Nutrition*, 37(5), 740–748.
- Havel, P. J. (2005). Dietary Fructose: Implications for Dysregulation of Energy Homeostasis and Lipid/Carbohydrate Metabolism. *Nutrition Reviews*, 63(5), 133–157.
- Heinz, F., Lamprecht, W., & Kirsch, J. (1968). Enzymes of fructose metabolism in human liver. *Journal of Clinical Investigation*, 47(8), 1826–1832.
- Hirahatake, K. M., Meissen, J. K., Fiehn, O., & Adams, S. H. (2011). Comparative Effects of Fructose and Glucose on Lipogenic Gene Expression and Intermediary Metabolism in HepG2 Liver Cells. *PLoS ONE*, 6(11), e26583.
- Ho, J. E., Larson, M. G., Vasan, R. S., Ghorbani, A., Cheng, S., Rhee, E. P., et al. (2013). Metabolite profiles during oral glucose challenge. *Diabetes*, 62(8), 2689–2698.
- Kanehisa, M., Goto, S., Furumichi, M., Tanabe, M., & Hirakawa, M. (2010). KEGG for representation and analysis of molecular networks involving diseases and drugs. *Nucleic Acids Research*, 38, D355–D360.
- Kind, T., Liu, K. H., Lee do, Y., DeFelice, B., Meissen, J. K., & Fiehn, O. (2013). LipidBlast in silico tandem mass spectrometry database for lipid identification. *Nature Methods*, 10(8), 755–758.
- Kind, T., Wohlgemuth, G., Lee, D. Y., Lu, Y., Palazoglu, M., Shahbaz, S., et al. (2009). FiehnLib: Mass Spectral and Retention Index Libraries for Metabolomics Based on Quadrupole and Time-of-Flight Gas Chromatography/Mass Spectrometry. *Analytical Chemistry*, 81(24), 10038–10048.
- Koo, H.-Y., Wallig, M. A., Chung, B. H., Nara, T. Y., Cho, B. H. S., & Nakamura, M. T. (2008). Dietary fructose induces a wide range of genes with distinct shift in carbohydrate and lipid metabolism in fed and fasted rat liver. *Biochimica et Biophysica Acta*, 1782(5), 341–348.
- Lee, d Y, Park, J. J., Barupal, D. K., Fiehn, O., & Lee, d Y. (2012). System response of metabolic networks in Chlamydomonas reinhardtii to total available ammonium. *Molecular and Cellular Proteomics*, 11(10), 973–988.
- Lei, Z., Huhman, D. V., & Sumner, L. W. (2011). Mass Spectrometry Strategies in Metabolomics. *Journal of Biological Chemistry*, 286(29), 25435–25442.
- Lin, S., Yang, Z., Liu, H., Tang, L., & Cai, Z. (2011). Beyond glucose: metabolic shifts in responses to the effects of the oral glucose tolerance test and the high-fructose diet in rats. *Molecular BioSystems*, 7(5), 1537–1548.

- Locasale, J. W. (2013). Serine, glycine and one-carbon units: cancer metabolism in full circle. *Nature Reviews Cancer*, 13(8), 572–583.
- Loenen, W. A. (2006). S-adenosylmethionine: jack of all trades and master of everything? *Biochemical Society Transactions*, 34(Pt 2), 330–333.
- Maret, W., & Auld, D. S. (1987). Purification and characterization of human liver sorbitol dehydrogenase. *Biochemistry*, 27(5), 1622–1628.
- Mayes, P. A. (1993). Intermediary metabolism of fructose. *The American Journal of Clinical Nutrition*, 58(5 Suppl), 754S–765S.
- McGarry, J. D., & Brown, N. F. (1997). The mitochondrial carnitine palmitoyltransferase system. From concept to molecular analysis. *European Journal of Biochemistry*, 244(1), 1–14.
- McGarry, J. D., & Foster, D. W. (1980). Regulation of hepatic fatty acid oxidation and ketone body production. *Annual Review of Biochemistry*, 49, 395–420.
- Mendeloff, A. I., & Weichselbaum, T. E. (1953). Role of the human liver in the assimilation of intravenously administered fructose. *Metabolism, Clinical and Experimental*, 2(5), 450–458.
- Parks, E. J., & Hellerstein, M. K. (2000). Carbohydrate-induced hypertriglycerolemia: historical perspective and review of biological mechanisms. *The American Journal of Clinical Nutrition*, 71(2), 412–433.
- Pluskal, T., Castillo, S., Villar-Briones, A., & Orešič, M. (2010). MZmine 2: Modular framework for processing, visualizing, and analyzing mass spectrometry-based molecular profile data. *BMC Bioinformatics*, 11, 395.
- Rizkalla, S. W. (2010). Health implications of fructose consumption: A review of recent data. *Nutrition & Metabolism*, 4(7), 82.
- Roglans, N., Sanguino, E., Peris, C., Alegret, M., Vázquez, M., Adzet, T., et al. (2002). Atorvastatin treatment induced peroxisome proliferator-activated receptor alpha expression and decreased plasma nonesterified fatty acids and liver triglyceride in fructose-fed rats. *Journal of Pharmacology and Experimental Therapeutics*, 302(1), 232–239.
- Scott, J. M. (1999). Folate and vitamin B12. *The Proceedings of the Nutrition Society*, 58(2), 441–448.
- Shannon, P., Markiel, A., Ozier, O., Baliga, N. S., Wang, J. T., Ramage, D., et al. (2003). Cytoscape: a software environment for integrated models of biomolecular interaction networks. *Genome Research*, 13(11), 2498–2504.
- Smith, C. A., O'Maille, G., Want, E. J., Qin, C., Trauger, S. A., Brandon, T. R., et al. (2005). METLIN: A metabolite mass spectral database. *Therapeutic Drug Monitoring*, 27(5), 747–751.
- Spence, J. T., & Pitot, H. C. (1982). Induction of lipogenic enzymes in primary cultures of rat hepatocytes. Relationship between lipogenesis and carbohydrate metabolism. *European Journal of Biochemistry*, 128(1), 15–20.
- Sun, S. Z., & Empie, M. W. (2012). Fructose metabolism in humans—what isotopic tracer studies tell us. *Nutrition & Metabolism (Lond)*, 9(1), 89.
- Tibbetts, A. S., & Appling, D. R. (2010). Compartmentalization of Mammalian folate-mediated one-carbon metabolism. *Annual Review of Nutrition*, 30, 57–81.
- Topping, D. L., & Mayes, P. A. (1971). The concentration of fructose, glucose and lactate in the splanchnic blood vessels of rats absorbing fructose. *Nutrition & Metabolism*, 13(6), 331–338.
- Topping, D. L., & Mayes, P. A. (1972). The immediate effects of insulin and fructose on the metabolism of the perfused liver. Changes in lipoprotein secretion, fatty acid oxidation and esterification, lipogenesis and carbohydrate metabolism. *The Biochemical Journal*, 126(2), 295–311.
- Umbarger, H. E. (1978). Amino acid biosynthesis and its regulation. *Annual Review of Biochemistry*, 47, 532–606.
- Underwood, A. H., & Newsholme, E. A. (1965). Properties of phosphofructokinase from rat liver and Their Relation to the control of glycolysis and gluconeogenesis. *The Biochemical Journal*, 95, 858–865.
- Vance, J. E. (2008). Phosphatidylserine and phosphatidylethanolamine in mammalian cells: two metabolically related aminophospholipids. *Journal of Lipid Research*, 49(7), 1377–1387.
- Vance, D. E., & Ridgway, N. D. (1988). The methylation of phosphatidylethanolamine. *Progress in Lipid Research*, 27(1), 61–79.
- Vilà, L., Roglans, N., Perna, V., Sánchez, R. M., Vázquez-Carrera, M., Alegret, M., et al. (2011). Liver AMP/ATP ratio and fructokinase expression are related to gender differences in AMPK activity and glucose intolerance in rats ingesting liquid fructose. *The Journal of Nutritional Biochemistry*, 22(8), 741–751.
- Wakil, S. J., Stoops, J. K., & Joshi, V. C. (1983). Fatty acid synthesis and its regulation. *Annual Review of Biochemistry*, 52, 579–837.
- Westerhuis, J. A., Hoefsloot, H. C. J., Smit, S., Vis, D. J., Smilde, A. K., van Velzen, E. J. J., et al. (2008). Assessment of PLS-DA cross validation. *Metabolomics*, 4(1), 81–89.
- Winder, W. W., Booth, F. W., Fitts, R. H., & Holloszy, J. O. (1975). Effect of exercise on response of liver lipogenic enzymes to a high fructose diet. *Proceedings of the Society for Experimental Biology and Medicine Society for Experimental Biology and Medicine*, 148(4), 1150–1154.